Tumor-Associated MICA Is Shed by ADAM Proteases

Inja Waldhauer,[1] Dennis Goehlsdorf,[1] Friederike Gieseke,[1] Toni Weinschenk,[1] Mareike Wittenbrink,[1] Andreas Ludwig,[2] Stefan Stevanovic,[1] Hans-Georg Rammensee,[1] and Alexander Steinle[1]

[1]Institute for Cell Biology, Department of Immunology, Eberhard-Karls-University, Tübingen, Germany and [2]Institute for Pharmacology and Toxicology, University Hospital RWTH Aachen, Aachen, Germany

Abstract

The immunoreceptor NKG2D promotes immunosurveillance of malignant cells and protects the host from tumor initiation by activating natural killer cells and costimulating CD8 T cells. NKG2D-mediated recognition of malignant cells by cytotoxic lymphocytes is enabled through the tumor-associated expression of NKG2D ligands (NKG2DL) resulting from cellular or genotoxic stress. Shedding of NKG2DL is thought to constitute a major countermechanism of tumor cells to subvert NKG2D-mediated immunosurveillance. Here, we report that the prototypical NKG2DL MICA is released by proteolytic cleavage in the stalk of the MICA ectodomain, where deletions, but not alanine substitutions, impede MICA shedding. Small compound-mediated stimulation and inhibition of MICA shedding adduced characteristics that indicated an involvement of members of the "a disintegrin and metalloproteinase" (ADAM) family. Accordingly, MICA shedding by tumor cells was inhibited by silencing of the related ADAM10 and ADAM17 proteases, which are known to promote tumor growth by releasing epidermal growth factor receptor ligands. Collectively, our data show that ADAM10 and ADAM17 are critically involved in the tumor-associated proteolytic release of soluble MICA facilitating tumor immune escape. Hence, therapeutic blockade of ADAM10 and ADAM17 seems promising for cancer treatment by targeting both growth and immune escape of tumors. [Cancer Res 2008;68(15):6368–76]

Introduction

In the past, a role of the immune system in the control of cancer has been controversially discussed, but evidence in support of an active tumor immunosurveillance is broadly accumulating. In particular, the concept of cancer immunoediting by Schreiber and colleagues provides an attractive blueprint to accommodate many experimental findings and clinical observations in the field of tumor immunology (1, 2). Accordingly, the interaction between cancer and immune system is characterized by three phases comprising initial immune-mediated tumor elimination, an equilibrium phase, and, finally, the evasion of tumors from immunosurveillance (1, 2). A major challenge remains to explain how the immune system is able to recognize malignant autologous cells and to mount an antitumor immune response in spite of the "self"-tolerance of the immune system. Work on the NKG2D/NKG2D ligand (NKG2DL) system has provided a novel rationale for the immune-mediated recognition of tumors because the activating receptor NKG2D endows cytotoxic effectors of both the innate and adaptive immune system with the capacity to detect and eliminate malignant cells (1–4).

NKG2D is a homodimeric, C-type lectin-like receptor expressed by virtually all human natural killer (NK) cells, CD8 αβ T cells, and γδ T cells and, in association with the adaptor protein DAP10, transduces activating signals, which stimulate cytotoxicity and cytokine secretion (5–7). A peculiarity of NKG2D is the remarkable number of stress-inducible NKG2DL, which typically are not expressed by healthy tissue but rather are induced subsequently to harmful events such as cellular stress or viral infection (7–10). Human NKG2DL belong to the families of MHC-encoded MIC molecules (MICA and MICB) and non–MHC-encoded UL16-binding proteins (ULBP; ULBP1, ULBP2, ULBP3, ULBP4, RAET1G, and RAET1L; refs. 7, 8, 11). In tumor cells, MICA and other NKG2DL are up-regulated by genotoxic stress dependent on the activity of the DNA damage-detecting protein kinase ataxia-telangiectasia mutated (3). Genotoxic stress often occurs in precancerous lesions and in many established tumors, and accordingly, MIC molecules are broadly expressed on epithelial tumors and on some hematopoietic malignancies (3, 12–14), suggesting that they act as "immuno-alerters" of malignant transformation. Studies in mice showed a potent stimulatory role of NKG2D in tumor immunity: NK and CD8 T cells readily eliminated tumor cells ectopically expressing NKG2DL in a NKG2D-dependent manner, thereby even inducing tumor immunity against the parental tumor cells (15–17). Further, NKG2D was also shown to protect from tumor initiation (18–20), rendering the NKG2D/NKG2DL system an interesting target for tumor immunotherapy.

In established MICA-expressing human tumors, NKG2D-mediated immunosurveillance is thought to be antagonized by the release of soluble MICA (sMICA) promoting tumor evasion by several independent mechanisms. This includes shedding-associated reduction of the overall surface density of NKG2DL on tumors as well as systemic NKG2D down-regulation on NK cells and CD8 T cells and expansion of immunosuppressive intratumoral $CD4^+NKG2D^+$ T cells by sMICA (21–24). Meanwhile, elevated levels of sMICA have been reported for sera of many cancer patients with a broad variety of different malignancies (13, 14, 22, 24, 25). Therefore, elucidating the molecular mechanisms of MICA shedding and, subsequently, development of therapeutic strategies to suppress MICA shedding may be of substantial benefit in cancer treatment. A recent study showed a critical and unprecedented contribution of the protein disulfide isomerase ERp5 to MICA shedding at the surface of tumor cells (26). ERp5 was shown to

Note: Supplementary data for this article are available at Cancer Research Online (http://cancerres.aacrjournals.org/).

Requests for reprints: Alexander Steinle, Institute for Cell Biology, Department of Immunology, Eberhard-Karls-University, Auf der Morgenstelle 15, D-72076 Tübingen, Germany. Phone: 49-7071-2980992; Fax: 49-7071-29-5653; E-mail: alexander.steinle@uni-tuebingen.de.

doi:10.1158/0008-5472.CAN-07-6768

form transitory disulfide complexes with the α3 domain of MICA and suggested to thereby induce a large conformational change enabling proteolytic cleavage of MICA (26). However, the nature of the protease(s) ultimately responsible for MICA shedding was not addressed by this study.

Previously, we had reported that release of sMICA as well as sMICB and sULBP2 from tumor cells is impaired by metalloproteinase inhibitors, pointing to an involvement of members of the metzincin superfamily, such as members of the families of matrix metalloproteinases (MMP) and "a disintegrin and metalloproteinase" (ADAM) proteins (24, 27, 28). Whereas MMPs are largely implicated in destruction of extracellular matrix, invasion of the basement membrane, and angiogenesis, many ADAMs are membrane-tethered proteases and one of their major functions is the proteolytic release of ectodomains of transmembranous proteins, including cytokines, growth factors, and cell adhesion molecules, from the cell surface (29–31). In particular, ADAM10 and ADAM17, also largely known as tumor necrosis factor (TNF)-α–converting enzyme (TACE), play an eminent role in the shedding of ectodomains. The catalytic domains of ADAM10 and ADAM17/TACE are related, and consequently, both metalloproteinases share some of their substrates such as amyloid precursor protein (APP) and TNF (29, 31, 32). Many ADAMs are frequently overexpressed in tumors and are thought to play key roles in different steps of tumorigenesis (31, 33).

Based on our observations that shedding of MIC molecules is blocked by metalloproteinase inhibitors, we set out to characterize the proteolytic activities involved in this process. We anticipated that molecular characterization of the responsible protease(s) may identify new promising targets in the quest for more efficacious immunotherapies of cancer.

Materials and Methods

Transfectants. The human B-cell line C1R was cultured in 10% FCS-RPMI 1640, C1R-MICA transfectants with additional 1.8 mg/mL G418, the human embryonic fibroblast cell line 293T and the cervix carcinoma cell line HeLa in 10% FCS-Iscove's modified Dulbecco's medium, and 293T-MICA, 293T-ULBP2, and HeLa-MICA transfectants with additional 1.5 mg/mL G418. 293T and HeLa were stably transfected with MICA*01 or ULBP2 cDNA using FuGene HD reagent (Roche), and C1R was transfected with cDNA of MICA mutants by electroporation as described (24). MICA mutants were generated from full-length MICA*01 cDNA (all in RSV.5neo) using QuikChange kit (Stratagene) and the following oligonucleotides: 1D, 5′-GGAAAGTGCTGGTGCTTCAGACATTCCATGTTTCTG-3′ and 5′-CAGAAACATGGAATGTCTGAAGCACCAGCACTTTCC-3′; 2D, 5′-CTCTGCCCTCTGGGTGGCAGACGTTCCATG-3′ and 5′-CATGGAATGTCTGCCACCCAGAGGGCAGAG-3′; 3D, 5′-CTGCCCTCTGGGGCTGTTGCTGCTGC-3′ and 5′-GCAGCAGCAACAGCCCCAGAGGGCAG-3′; 1M, 5′-CTGCCCTCTGGGAAAGCGGCGGCGGCTCAGAGTCATTGGCAG-3′ and 5′-CTGCCAATGACTCTGAGCCGCCGCCGCTTTCCCAGAGGGCAG-3′; 2M, 5′-GGGAAAGTGCTGGTGCTTGCGGCTCATTGGCAGACGTTCCAT-3′ and 5′-ATGGAATGTCTGCCAATGAGCCGCAAGCACCAGCACTTTCCC-3′; 3M, 5′-GTGCTGGTGCTTCAGAGTGCTGCGCAGACGTTCCATGTTTCTGC-3′ and 5′-GCAGAAACATGGAATGTCTGCGCAGCACTCTGAAGCACCAGCAC-3′; 4M, 5′-GTGCTTCAGAGTCATTGGGCGGCATTCCATGTTTCTGCTG-3′ and 5′-CAGCAGAAACATGGAATGCCGCCCAATGACTCTGAAGCAC-3′; 5M, 5′-CAGAGTCATTGGCAGACAGCCGCTGTTTCTGCTGTTGCTGCTG-3′ and 5′-CAGCAGCAACAGCAGAAACAGCGGCTGTCTGCCAATGACTCTG-3′; and 6M, 5′-GGCAGACATTCCATGCTGCTGCTGTTGCTGCTGC-3′ and 5′-GCAGCAGCAACAGCAGCATGGAATGTCTGCC-3′.

Reagents. Phycoerythrin (PE)-labeled human NKG2D tetramers, anti-MICA monoclonal antibody (mAb) AMO1, anti-MICA/MICB mAb BAMO1 and BAMO3, and anti-ULBP2 BUMO1 were previously described (10). Antibodies specific for human ADAM10 (mAb 163003) and human ADAM17 (mAb 111633) were from R&D Systems. Horseradish peroxidase (HRP)-goat anti-mouse Ig, HRP-streptavidin, and PE-goat anti-mouse Ig were from Jackson ImmunoResearch Laboratories. HRP-goat anti-mouse IgG2a was from Southern Biotechnology Associates. MMP inhibitor III (MMPI III), tissue inhibitor of metalloproteinases 2 (TIMP2), and bisindolylmaleimide I (BIM I) were from Merck. BB94 (a kind gift of Klaus Maskos, Max-Planck-Institute for Biochemistry, Martinsried, Germany) was dissolved in dimethylformamide and added in a 1:200 volume to cell cultures. ADAM-specific metalloproteinase inhibitors GW280264X and GI254023X were previously described (34). Phorbol 12-myristate 13-acetate (PMA) was from Cell Signaling and carboxyfluorescein diacetate succinimidyl ester (CFSE) was from Sigma.

Flow cytometry. Cells were incubated with indicated antibodies (10 μg/mL) and then, after washing, stained with PE-goat anti-mouse Ig (1:200 dilution) as secondary reagent or, alternatively, with PE-labeled soluble NKG2D (sNKG2D) tetramers (10 μg/mL). Samples were analyzed on a FACScan (BD Biosciences). Specific fluorescence intensities (SFI) were calculated by subtracting the mean fluorescence intensity (MFI) of the isotype control from the MFI of the specific antibody.

ELISA. The sandwich ELISA for sMICA based on the MICA-specific capture mAb AMO1 (IgG1) and the MICA/MICB-specific sandwich mAb BAMO3 (IgG2a) has been previously described (13). BAMO3 binding was detected with HRP-conjugated anti-mouse IgG2a and plates were developed using the Tetramethylbenzidine Peroxidase Substrate System (KPL). The sandwich ELISA for sULBP2 based on the ULBP2-specific mAb BUMO1 (capture mAb, IgG1) and mAb 165903 (sandwich mAb, IgG2a; R&D Systems) was performed as previously reported (28). Results are shown as means with SD of triplicates.

Immunoblot analysis. For cell surface biotinylation, 293T-MICA cells were washed with PBS and subsequently incubated with 1 mg/mL EZ-Link Sulfo-NHS-LC-Biotin (Pierce) for 20 min at room temperature. The reaction was stopped by washing twice with 100 mmol/L glycine and once with PBS. Samples were separated by 10% SDS-PAGE. Gels were blotted to Hybond-enhanced chemiluminescence membranes (Amersham), blocked with TBS containing 5% nonfat dried milk, and then analyzed for MICA with anti-MICA/MICB mAb BAMO1 followed by a goat anti-mouse HRP conjugate or for biotinylated proteins with HRP-conjugated streptavidin and developed with SuperSignal West Pico Chemiluminescent Substrate (Pierce).

Proliferation analysis. For proliferation analysis, 293T-MICA cells were labeled with 5 μmol/L CFSE 48 h after transfection, washed, and cultured for an additional 4 d before flow cytometric analysis.

Determination of COOH terminus of sMICA. Supernatants from C1R-MICA were concentrated, dialyzed, and treated with peptide:*N*-glycanase F (New England Biolabs) according to the manufacturer's instructions. Deglycosylated sMICA was immunoprecipitated with mAb BAMO3, separated on a 12.5% SDS-PAGE, and stained with Coomassie blue. sMICA was excised from the gel and digested with V8 protease (Roche) in the presence of H_2O^{18} (Campro Scientific). After digestion, the fragments were extracted once with 1% formic acid and twice with 50% methanol, and resulting fragments were analyzed by matrix-assisted laser desorption/ionization-mass spectrometry (MALDI-MS).

RNA silencing. For transient knockdown of human ADAM10, oligonucleotide 5′-ACAGTGCAGTCCAAGTCAA-3′ and its reverse complement, separated by a 9-nucleotide hairpin spacer (ttcaagaga), were inserted into the expression vector pSuper-puro (35). 293T-MICA cells were transfected with pSuper-puro or pSuper-ADAM10 and, 72 h after transfection, analyzed for constitutive MICA shedding. For direct delivery of small interfering RNA (siRNA), 293T-MICA, HeLa-MICA, or 293T-ULBP2 cells were transfected with ADAM17 and/or ADAM10 ON-TARGETplus SMARTpools (Dharmacon) using DharmaFECT1 (Dharmacon). The following oligonucleotides were used: ADAM17, 5′-GAAGAACACGUGUAAAUUAUU-3′, 5′-GCACAAAGAAUUAUGGUAAUU-3′, 5′-UAUGGGAACUCUUGGAUUAUU-3′, and 5′-GGAAAUAUGUCAUGUAUCCUU-3′; ADAM10, 5′-CAUCUGACCCUAAACCAAAUU-3′, 5′-CAAGGGAAGGAAUAUGUAAUU-3′, 5′-GAACUAUGGGUCUCAUGUAUU-3′, and 5′-CGAGAGAGUUAUCAAAUGGUU-3′. As a control,

ON-TARGETplus siCONTROL nontargeting pool (Dharmacon) was used. Shedding of MICA or ULBP2 was analyzed 72 h after transfection by ELISA.

Real-time reverse transcription-PCR. Total RNA was isolated using Trizol (Invitrogen) followed by DNase I (Promega) digestion and reverse transcription using Moloney murine leukemia virus reverse transcriptase (Promega). Resulting cDNA was amplified with ADAM10-, ADAM17-, MICA-, and 18S rRNA–specific primers (40 cycles, 95°C for 15 s, 60°C for 1 min) using SYBR Green chemistry on the ABI PRISM 7000 Sequence Detection System (Applied Biosystems). The ΔC_T method was used for relative quantifications. Oligonucleotide sequences were as follows: 18S rRNA, 5′-CGGCTACCACATCCAAGGAA-3′ (forward) and 5′-GCTGGAATTACCGCGGCT-3′ (reverse); MICA, 5′-CCTTGGCCATGAACGTCAGG-3′ (forward) and 5′-CCTCTGAGGCCTCRCTGCG-3′ (reverse); ADAM10, 5′-CTGGCCAACCTATTTGTGGAA-3′ (forward) and 5′-GACCTTGACTTGGACTGCACTG-3′ (reverse); and ADAM17, 5′-GAAGGCCAGGAGGCGATTA-3′ (forward) and 5′-CGGGCACTCACTGCTATTACC-3′ (reverse).

Statistics. Analysis of significance was performed with Student's *t* test using SigmaStat software.

Results

COOH-terminus of sMICA. Previously, we showed that sMICA in culture supernatants of MICA-expressing tumor cells is markedly smaller than the membrane-associated form of MICA but comparable in size to MICA ectodomains recombinantly produced in *Escherichia coli* (24). In conjunction with our finding that release of sMICA from tumor cells is blocked by metalloproteinase inhibitors, we predicted that sMICA comprises the entire MICA ectodomain generated by proteolytic cleavage of membrane-bound MICA by one or several metalloproteinases. To further characterize the generation of tumor cell–derived sMICA, COOH termini of sMICA purified from supernatants of C1R-MICA cells were determined by MALDI-MS after proteolytic digestion in the presence of H_2O^{18} (Fig. 1*A*). We found staggered COOH termini that all mapped to the stalk region (Ser^{274} to Ala^{291}) connecting the MICA α3 domain and the transmembrane domain (Fig. 1*B*).

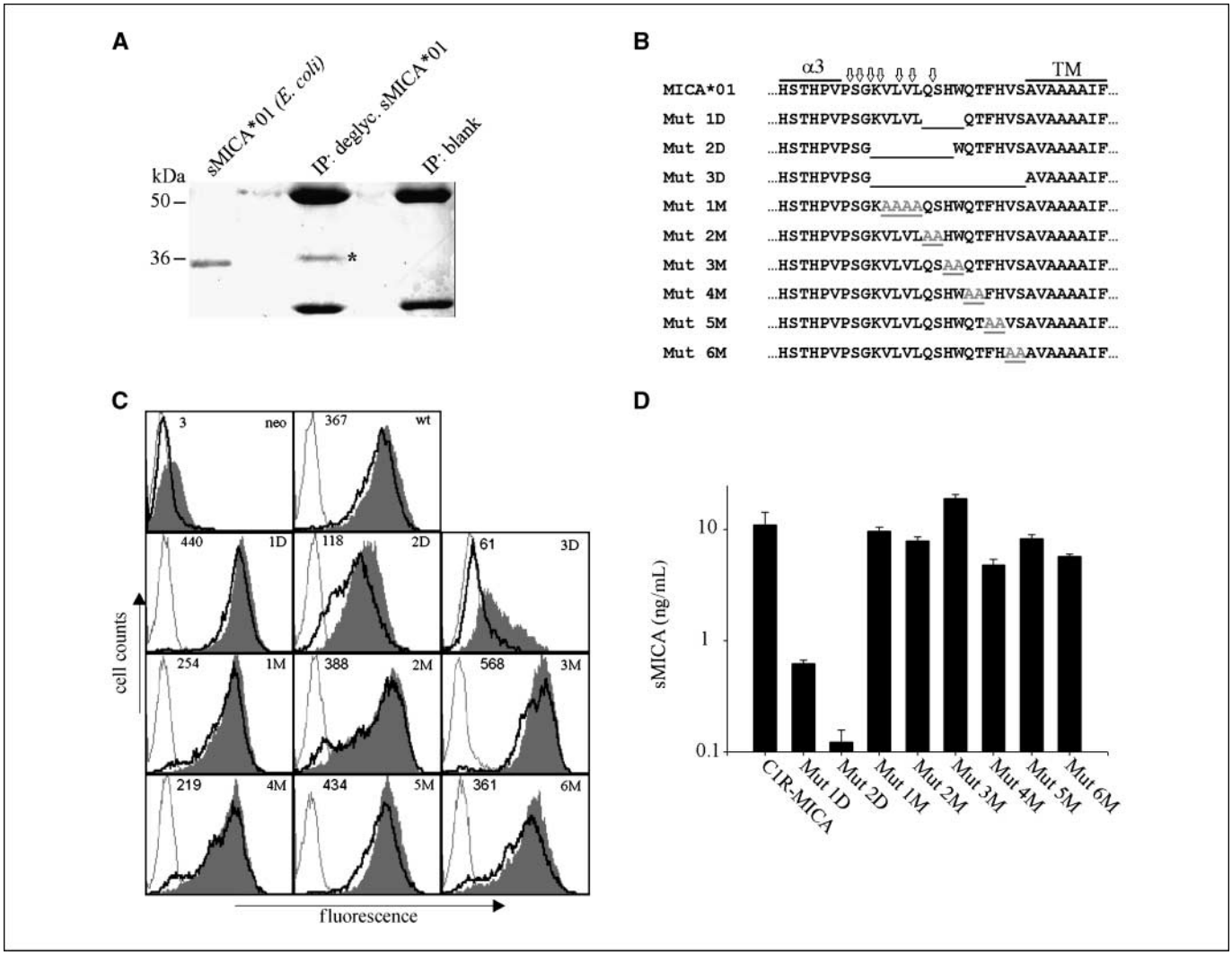

Figure 1. MICA cleavage in the stalk region is dependent on the length but not on the sequence of the stalk. *A,* tumor cell–shed sMICA (*asterisk, middle*) from *N*-glycanase–treated supernatants of C1R-MICA*01 cells was immunoprecipitated (*IP*) with mAb BAMO3 for MS analysis. *E. coli*–produced sMICA*01 (*left lane*) and a mock immunoprecipitation (*right lane*) are controls. *B,* sequence of the MICA stalk connecting the α3 and the transmembrane domain (*TM*) where vertical arrows indicate COOH termini of shed sMICA as determined by MS (*top line*). *Bottom lines,* mutant MICA sequences with deletions (1D to 3D) or alanine substitutions (1M to 6M), respectively, transfected into C1R cells. *C,* C1R cells stably transfected with MICA*01 mutants, wild-type MICA*01 (*wt*), or mock-transfected C1R cells (*neo*) were stained with anti-MICA mAb AMO1 (*filled histograms*), isotype control IgG1 (*gray lines*), or sNKG2D tetramers (*solid lines*). SFI values of AMO1 stainings are indicated in the top left corner of the respective histograms. Mock-transfected C1R cells only express marginal levels of MICA and are not stained by NKG2D tetramers. *D,* sMICA in supernatants of C1R cells stably expressing MICA mutants was determined after 16 h of cultivation using a sMICA-specific sandwich ELISA. No sMICA was detectable in supernatants of C1R-neo and C1R-Mut 3D transfectants (data not shown).

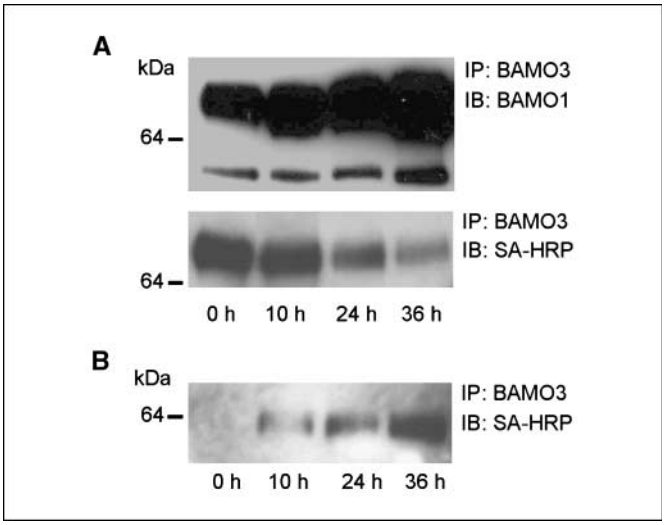

Figure 2. MICA is shed from the cell surface. *A* and *B,* 293T-MICA cells were surface biotinylated and cultivated for up to 36 h before MIC molecules in cell lysates (*A*) or culture supernatants (*B*) were immunoprecipitated by mAb BAMO3. Biotinylated MICA or total MICA molecules were then detected with streptavidin-HRP (*SA-HRP*) and anti-MIC mAb BAMO1, respectively.

Staggered COOH termini may be due to variable cleavage sites, secondary cleavages, as described for APP, or exopeptidase activity during sample processing. At any rate, these data show that sMICA comprises the entire ectodomain, including α1, α2, and α3 domain, and strongly support the notion that sMICA is generated from transmembranous MICA by proteolytic cleavage atop of the plasma membrane.

Efficiency of MICA shedding depends on the length of juxtamembranous stalk region. To further investigate mechanisms of proteolytic MICA cleavage, two types of mutants of the MICA stalk region were generated: (*a*) deletions of 4, 8, or 15 amino acids, respectively, and (*b*) substitutions where pairs of two adjacent amino acids (except mutant 1M: exchange of four amino acids) were replaced by alanines (Fig. 1*B*). C1R cells were stably transfected with this set of MICA mutants and analyzed for MICA surface expression, NKG2D binding, and sMICA release. All MICA mutants with alanine substitutions were expressed on the cell surface at nearly the same level as wild-type MICA. In contrast, only surface expression of mutant 1D was at wild-type levels, whereas surface expression of the other two deletion mutants was slightly (Mut 2D) or strongly (Mut 3D) impaired, suggesting that larger deletions of the stalk region adversely affect MICA surface expression (Fig. 1*C*). When MICA mutants were analyzed for NKG2D binding using sNKG2D tetramers, stainings were comparable with stainings with the MICA-specific antibody AMO1, indicating that MICA mutants expressed at the cell surface were not conformationally altered (Fig. 1*C*). Subsequently, we analyzed supernatants of transfected C1R cells for sMICA using our previously established sMICA ELISA (Fig. 1*D*; ref. 13). Whereas alanine substitutions in the MICA stalk did not substantially affect MICA shedding, sMICA levels in supernatants of C1R cells expressing mutants 1D and 2D were reduced more than 10-fold or to background levels, respectively. These results show that the protease(s) responsible for MICA shedding do(es) not recognize a specific sequence motif within the stalk but rather is (are) sensitive to shortenings of the stalk region separating the MICA α3 domain from the plasma membrane.

MICA is shed from the cell surface. Next, we attempted to define the cellular compartment where MICA shedding occurs. Hence, cell surface proteins of 293T-MICA cells were biotinylated, and subsequently, both cell lysates and supernatants were analyzed

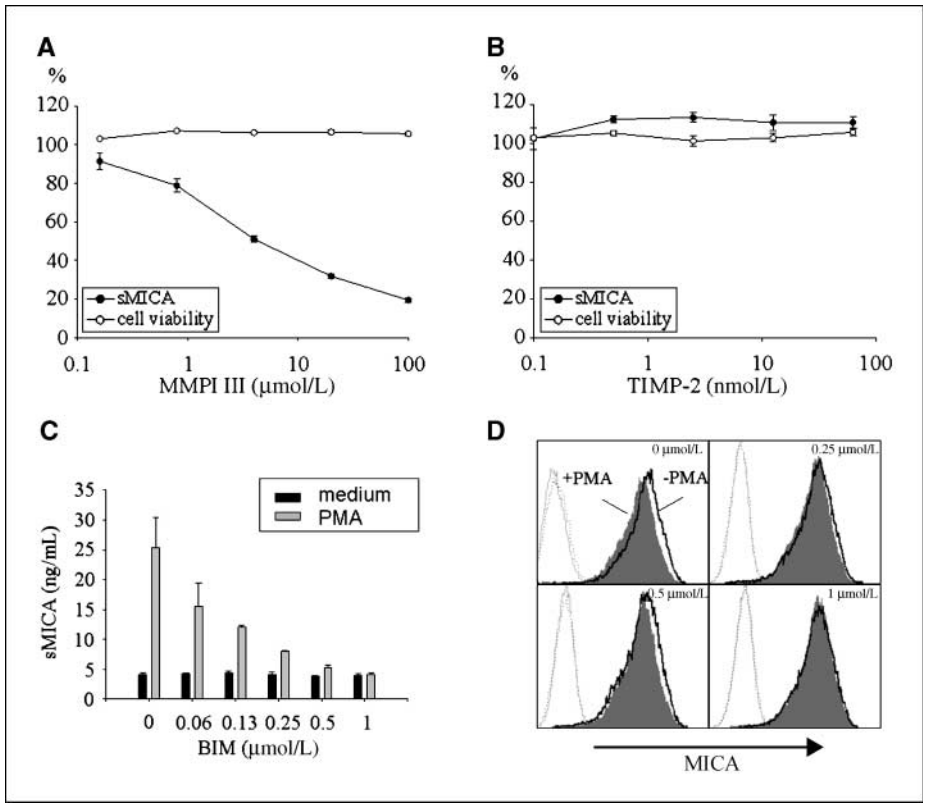

Figure 3. Chemical inhibition of MICA shedding reveals characteristics of ADAM-dependent proteolysis. *A* and *B,* MICA shedding by C1R-MICA cells is repressed by the broad metalloproteinase inhibitor MMPI III in a concentration-dependent manner (*A*) but not by the natural MMP-specific inhibitor TIMP2 (*B*). Cellular viability was monitored by propidium iodide staining. *C,* PMA-stimulated shedding of MICA by C1R-MICA cells was efficiently blocked by preincubation with the PKC inhibitor BIM I. *D,* PMA-stimulated MICA shedding and the BIM I–mediated inhibition is mirrored by alterations of cell surface MICA levels on C1R-MICA cells. C1R-MICA cells pretreated with various concentrations of BIM I were cultured with (*gray histograms*) or without (*white histograms*) PMA and stained with mAb AMO1. In *A* to *C*, levels of sMICA (MICA shedding) were determined by sMICA ELISA. PMA was used at 100 ng/mL in *C* and at 50 ng/mL in *D*.

for biotinylated MICA at different time points. To this aim, MICA was immunoprecipitated from lysates or supernatants by anti-MICA/MICB mAb BAMO3 followed by immunoblotting. Importantly, biotinylated MICA was found not only in cell lysates but also in supernatants, indicating that sMICA is shed from the cell surface (Fig. 2). Whereas the amount of biotinylated MICA in cell lysates decreased over time inversely to total MICA, biotinylated sMICA in the supernatant increased. Earlier studies had shown that sMICA and sMICB are rather stable in culture medium (27).

Inhibition of MICA shedding by broad-range metalloproteinase inhibitors. Next, we evaluated several broad-range metalloproteinase inhibitors for their ability to inhibit MICA shedding. MMPI III, which is known to inhibit a large number of metalloproteinases, strongly suppressed MICA shedding by C1R-MICA without affecting cell viability (Fig. 3*A*). Similar results were obtained for the inhibitors BB94, MMPI II, and GM6001 (data not shown; ref. 28). In contrast, TIMP2, a natural and selective inhibitor of MMPs that does not inhibit ADAMs (36), did not affect MICA shedding (Fig. 3*B*).

Protein kinase C stimulates MICA shedding. Previously, we had shown that MICA shedding is stimulated by PMA (28), a characteristic feature of ADAM17-mediated shedding (37). PMA-mediated activation of MICA shedding suggested the involvement of protein kinase C (PKC), which we further addressed by applying the PKC inhibitor BIM I. To this aim, we treated C1R-MICA with PMA and BIM I and analyzed supernatants for sMICA levels (Fig. 3*C*) and monitored cell surface MICA by flow cytometry (Fig. 3*D*). In fact, PMA-stimulated shedding was inhibited by BIM I in a dose-dependent manner and, at highest BIM I concentrations, reduced to levels of constitutive MICA shedding, whereas BIM I had no effect on MICA shedding of control-treated C1R-MICA cells. These data showed that MICA shedding is executed by one or several plasma membrane–bound protease(s) with at least one being stimulated by PKC.

MICA shedding is blocked by ADAM-specific inhibitors. Because our results pointed to the involvement of ADAMs in MICA shedding, we studied the effect of ADAM-specific hydroxamate-based metalloproteinase inhibitors on MICA shedding. The inhibitor GW280264X reportedly blocks proteolytic activity of both ADAM10 and ADAM17 with comparable efficiency, whereas GI254023X is ~100-fold more effective in blocking ADAM10 than ADAM17 (34). Shedding of MICA from unstimulated or PMA-stimulated C1R-MICA cells was efficiently inhibited by GW280264X in a dose-dependent manner (Fig. 4*B*). In contrast, GI254023X strongly inhibited constitutive shedding from unstimulated cells but only modestly affected shedding from PMA-stimulated cells (Fig. 4*A*). In all experiments, MICA shedding was efficiently blocked by the broad-range metalloproteinase inhibitor BB94 (data not shown). Collectively, our data suggested that MICA shedding is governed by one or several membrane-bound proteases with ADAM-like activities, such as ADAM10 and ADAM17.

ADAM10 and ADAM17 mediate MICA shedding. To directly address an involvement of ADAM10 and ADAM17 in MICA shedding, we transiently silenced the expression of ADAM10 and/or ADAM17 in 293T and HeLa cells by RNA interference. Because sMICA derived from endogenously expressed MICA could not be detected during the short, transient state of the ADAM knockdown (data not shown), we established 293T-MICA and HeLa-MICA cells ectopically expressing high levels of MICA*01. First, we suppressed ADAM10 by transfecting a plasmid expressing an ADAM10 siRNA (pSuper-ADAM10) into 293T-MICA cells. Down-regulation of ADAM10 transcripts was monitored by real-time PCR and of ADAM10 protein by immunoblotting (Fig. 5*A* and *B*). In flow cytometry, a strong down-regulation of ADAM10 surface expression was observed by ~65% of 293T-MICA cells at 72 h after transfection (Fig. 5*C*). To assess the effect of ADAM10 silencing on MICA shedding, we analyzed supernatants from pSuper-ADAM10–transfected or pSuper-puro–transfected 293T-MICA cells for sMICA. Levels of sMICA in 72- to 75-h posttransfection supernatants of pSuper-ADAM10–transfected cells were reduced by ~50% compared with sMICA levels of mock-transfected cells or comparable supernatants of untreated 293T-MICA cells (Fig. 5*D*). Similar results were obtained in three repeat experiments where sMICA levels were reduced by 31%, 49%, and 51%, respectively, with percentages of ADAM10 down-regulated cells ranging between 65% and 72% (data not shown). Noteworthy, levels of MICA transcripts and MICA surface expression remained unaltered (Fig. 5). To assess whether reduced sMICA levels may be due to an impaired proliferation as a consequence of ADAM10 knockdown, pSuper-puro–transfected and pSuper-ADAM10–transfected cells were labeled with CFSE and analyzed by flow cytometry after 4 days of culture (Supplementary Fig. S1). No difference in proliferation was observed between controls and ADAM10 knockdown cells. Altogether, these data showed that ADAM10 is crucially involved in constitutive shedding of MICA.

In a second approach, we transfected 293T-MICA cells with pools of siRNA targeting ADAM10 and/or ADAM17, respectively, to further analyze an involvement of ADAM10 and ADAM17 in MICA shedding. Successful siRNA-mediated suppression of ADAM expression was again confirmed by real-time PCR and flow cytometry (Fig. 6*A*; Supplementary Fig. S2). In 293T-MICA cells,

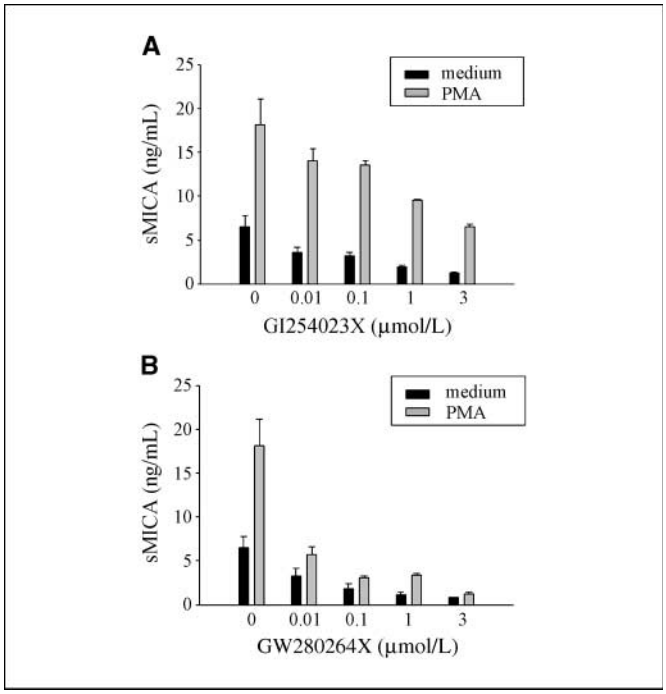

Figure 4. Inhibition of MICA shedding by ADAM-specific inhibitors. *A* and *B*, PMA-induced MICA shedding by C1R-MICA cells was potently inhibited by the ADAM protease inhibitor GW280264X (*B*) but only inefficiently by the selective ADAM protease inhibitor GI254023X (*A*), whereas both substances equally inhibited constitutive MICA shedding. Levels of sMICA were determined by sMICA ELISA and PMA was used at 100 ng/mL.

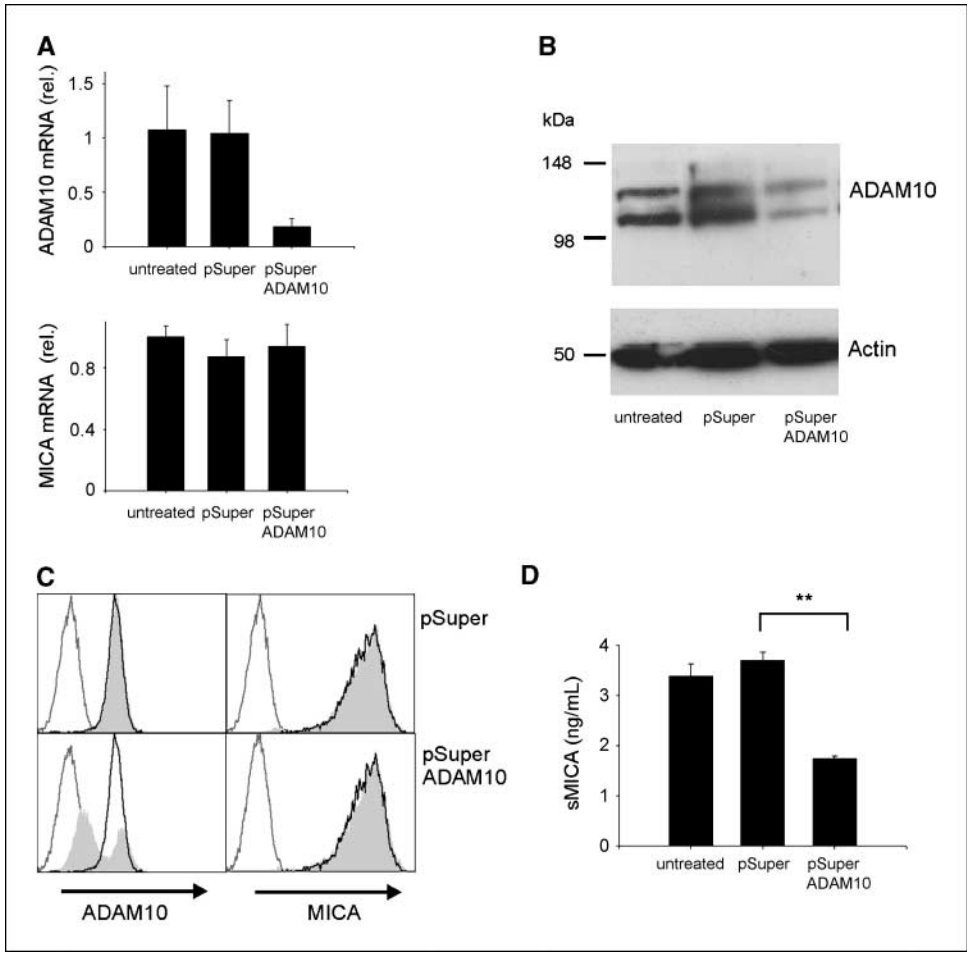

Figure 5. ADAM10 silencing impairs constitutive MICA shedding. *A* to *C,* ADAM10 siRNA expression in 293T-MICA cells down-regulates ADAM10 transcripts and total and cell surface ADAM10 protein expression. *A,* relative copy numbers of ADAM10 and MICA transcripts in 293T-MICA cells 48 h after transfection with pSuper-puro or pSuper-ADAM10 and in untreated 293T-MICA were determined by real-time PCR after normalization with 18S rRNA. *B,* total cellular ADAM10 protein was determined in lysates of 293T-MICA cells 72 h after transfection and of untreated 293T-MICA cells by immunoblotting. *C,* surface expression of MICA or ADAM10 (*gray histograms*) was determined 72 h after transfection. Overlays are respective stainings of untreated 293T-MICA cells (*thick lines*) and isotype control stainings of transfected 293T-MICA cells (*thin lines*). *D,* sMICA released from 293T-MICA transfected with pSuper or pSuper-ADAM10 was determined by sMICA ELISA in medium used for culture from 72 to 75 h after transfection and compared with 3-h culture supernatants of untreated 293T-MICA. **, $P < 0.001$.

constitutive MICA shedding was significantly reduced on knockdown of ADAM10 or a combined knockdown of ADAM10 and ADAM17 knockdown, whereas PMA-stimulated shedding was markedly reduced when either ADAM10 or ADAM17 was silenced (Fig. 6*B* and *C*). Targeting these ADAMs in HeLa-MICA cells also resulted in a diminished cell surface expression of ADAM10 and largely suppressed ADAM17 expression (Fig. 6*A*). Similar to 293T-MICA cells, suppressing ADAM10 expression resulted in a significant reduction of constitutive and PMA-stimulated MICA shedding. Notably, the efficient silencing of ADAM17 in HeLa-MICA cells not only impaired constitutive MICA shedding but even reduced shedding from PMA-stimulated cells by >85%. Cosilencing of ADAM10 and ADAM17 further suppressed PMA-stimulated MICA shedding to almost background levels (Fig. 6*B* and *C*).

Finally, we addressed an involvement of ADAM proteases in the previously reported proteolytic shedding of the glycosylphosphatidylinositol-anchored NKG2DL ULBP2 (28). We found that siRNA-mediated silencing of ADAM10 and/or ADAM17 in 293T-ULBP2 cells also impaired shedding of ULBP2 (Supplementary Fig. S3). Analogous to our observations for MICA shedding, ADAM17 has a greater effect on PMA-stimulated ULBP2 shedding than ADAM10.

Discussion

MICA shedding is considered a principal mechanism of tumor cells to escape from NKG2D-mediated immunosurveillance in humans. MICA shedding not only results in a reduction of MICA surface density on tumor cells but also generates sMICA, which was shown to systemically down-regulate NKG2D on cytotoxic effector cells and to promote expansion of immunosuppressive, intratumoral $CD4^+NKG2D^+$ T cells (13, 22–24). Thus, inhibition of MICA shedding represents a reasonable strategy to enhance antitumor immunity therapeutically. However, intelligent targeting of the MICA shedding process requires a thorough elucidation of the underlying molecular mechanisms. Previously, we had already shown that shedding of MICA as well as shedding of NKG2DL MICB and ULBP2 can be blocked by broad-range metalloproteinase inhibitors (24, 27, 28). But the nature of the proteases releasing sMICA remained unidentified.

Here, we report several lines of evidence that ADAM10 and ADAM17 act as principal sheddases of tumor cell–associated MICA: (*a*) MICA cleavage occurs at the surface of tumor cells, (*b*) MICA is cleaved within the juxtamembranous stalk, (*c*) MICA cleavage is dependent on the length but not on the sequence of the stalk, (*d*) MICA shedding is inhibited by broad-range metalloproteinase inhibitors but not by MMP-specific TIMP2, (*e*) MICA shedding is induced by PKC, (*f*) constitutive and induced MICA shedding is variably affected by ADAM-specific inhibitors GI254023X and GW280264X, and (*g*) shedding of MICA (and ULBP2) is suppressed on silencing of ADAM10 and/or ADAM17.

All these findings are in accord with well-known characteristics of ADAM activities: ADAMs typically release cell surface proteins through cleavage within the stalk region proximal to the membrane and select their substrates not by recognition of

consensus sequences but rather are guided by secondary structures also involving length and accessibility of the stalk (32, 38). Similarly to our observations for shedding of MICA and ULBP2, it has previously been reported for several other ADAM substrates [e.g., fractalkine, CD171, and epidermal growth factor receptor (EGFR) ligands] that shedding induced by phorbol esters involves ADAM17, whereas constitutive cleavage by unstimulated cells is mainly mediated by ADAM10 (37, 39, 40).

In most of our experiments, silencing of ADAM10 and/or ADAM17 resulted in a partial suppression of MICA shedding, which presumably is due to the incomplete silencing of the expression of these ADAM proteases in our transient experimental setting. For example, suppression of ADAM10 expression in about 65% to 72% of 293T-MICA cells was paralleled by a reduction of sMICA release by 31% to 50% (Fig. 5). An efficient suppression of ADAM17 in HeLa-MICA cells also strongly impaired PMA-stimulated MICA shedding (Fig. 6). However, it remains a possibility that other proteases additionally contribute to MICA shedding.

ADAMs are often up-regulated by tumor cells and are critically involved in promoting tumor growth and metastasis. In tumor cells, ADAM10 and ADAM17 provide growth factors such as EGF, transforming growth factor α (TGFα), and heparin-binding EGF, all ligands of EGFRs, which are important regulators of cell proliferation and survival (29, 33, 37). In human breast cancers, expression of ADAM17/TACE and TGFα was highly correlated and predictive of poor prognosis (41). Hence, targeting ADAM10 and/or ADAM17 in malignant diseases seems promising. In particular, targeting ADAM17 results in a broad inhibition of ligand release, which would be favorable in cancer treatment and may provide a clinical benefit (41, 42). The chronic bioavailability of TNF released by ADAM17 has also been associated with enhanced invasive activities and survival of neoplastic cells (43). *In vivo*, activity of ADAMs as well as MMPs is inhibited by TIMPs. In vertebrates, there exist four TIMPs that block MMPs and ADAMs through binding to the active site in a 1:1 stoichiometric fashion (44), except TIMP2, which does not affect ADAMs (36). It was shown that TIMP3 inhibits tumor growth *in vivo* (45), but many primary tumors lack detectable levels of TIMP3 due to aberrant DNA hypermethylation and this correlates with disease progression (46). Loss of TIMP3 expression in activated stromal cells enforces inflammation, enhances angiogenesis, and elicits rapid tumor development (43).

Small synthetic hydroxamate-based substances are also able to inhibit ADAMs. The crystal structure of ADAM17 in combination

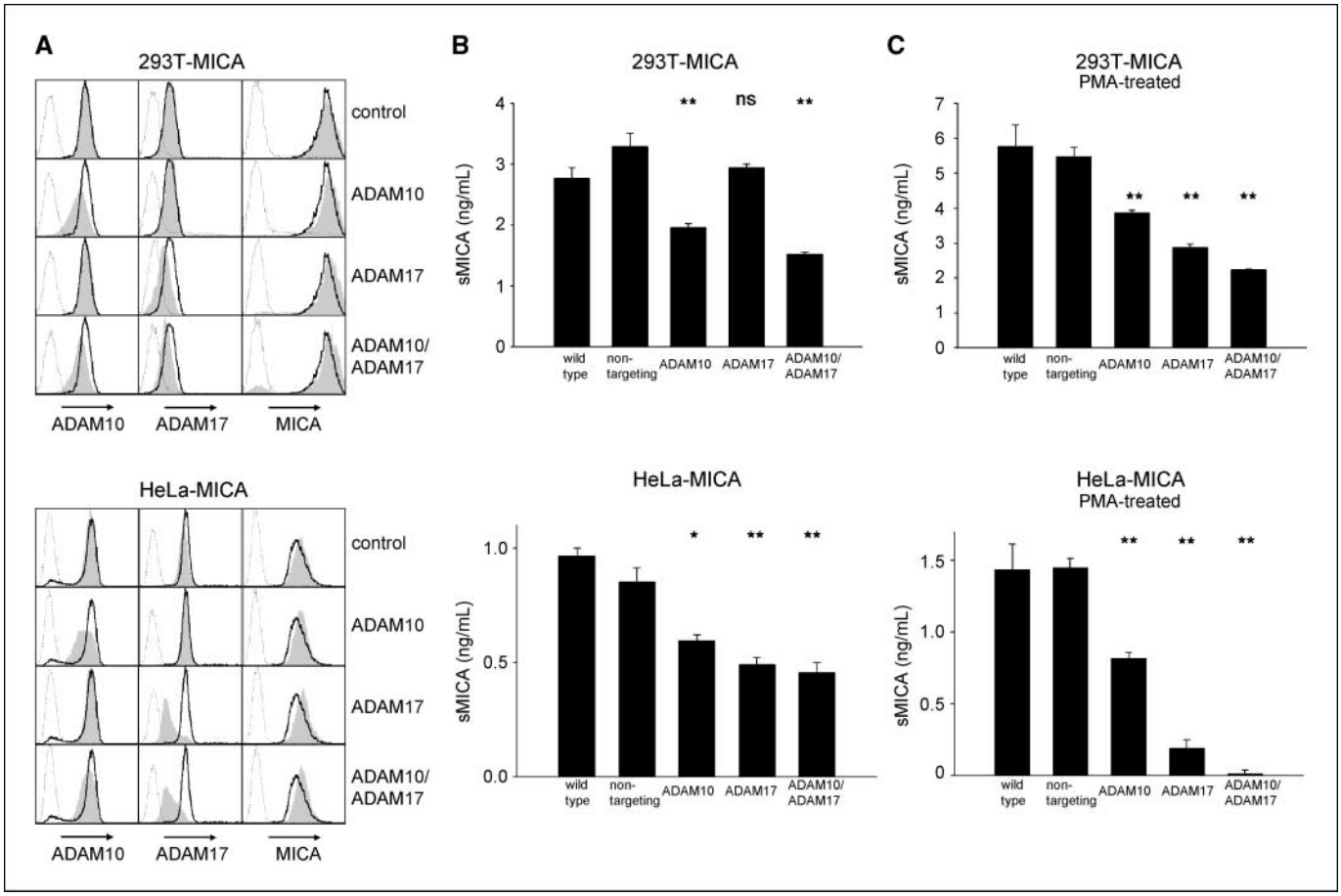

Figure 6. ADAM17 mediates PMA-stimulated MICA shedding. *A,* transient knockdown of ADAM10 and/or ADAM17 in 293T-MICA and HeLa-MICA cells by transfection of siRNA results in decreased levels of cell surface ADAM10 and/or ADAM17. Stainings of MICA, ADAM10, and ADAM17 (*gray histograms*) 72 h after transfection with control siRNA (nontargeting), ADAM10 siRNA, ADAM17 siRNA, or a mixture of ADAM10/ADAM17 siRNA are overlayed with stainings of untreated cells (*thick lines*) and isotype controls (*dotted lines*). Histograms show cells that have not been treated with PMA. *B* and *C,* levels of sMICA were determined by sMICA ELISA in supernatants 72 to 75 h after transfection (*B*) and after subsequent PMA treatment (100 ng/mL) at 75 h after transfection (supernatants of 75–77.5 h after transfection; *C*). *, $P = 0.003$; **, $P < 0.001$. *ns,* not significant. Significance was calculated for difference to control-treated (nontargeting siRNA treated) cells.

with such an inhibitor shows that the inhibitor blocks the active site and presumably replaces a water molecule in the active enzyme (32). Hydroxamate-based inhibitors such as batimastat (BB94) and marimastat (BB2516) were previously used in clinical trials (47, 48) but turned out to be inefficient or caused side effects by undesirable inhibition of nontarget ADAMs and MMPs (30, 49). There now exist novel compounds such as GI254023X, GW280264X, INCB7839, and INCB3619, which preferentially inhibit ADAM family members, including ADAM10 and ADAM17 (34, 50). To assess the effect on EGFR-mediated tumor growth, INCB3619 is currently evaluated in preclinical testing (50).

Our present study shows that suppression of ectodomain shedding by ADAM10 and ADAM17 also interferes with MICA and ULBP2 shedding from tumor cells and thereby is expected to hinder escape from NKG2D-mediated immunosurveillance. Hence, it is of great interest to determine whether treatment with these novel ADAM-specific inhibitors also results in an enhanced tumor immunity against NKG2DL-bearing tumors. The thioreductase ERp5 was shown to play an essential role in MICA shedding (26) presumably by chaperoning conformational alterations of surface MICA that may render MICA susceptible for proteolytic cleavage. Presently, it is unclear how activities of ADAMs and ERp5 interrelate in the MICA shedding process, but one may envision that chaperoning functions of ERp5 prepare surface MICA for proteolytic shedding by ADAMs. Further studies (e.g., in transgenic animal models) are necessary to establish whether targeting ADAMs or ERp5 results in reduced sMICA levels and an enhanced NKG2D-mediated tumor elimination.

Taken together, our study provides strong evidence that ADAM10 and ADAM17 are principal MICA sheddases on tumor cells. Hence, therapeutic targeting of ADAM10 and ADAM17 in cancer patients may be beneficial in terms not only of suppressing tumor growth but also by augmenting tumor immunogenicity.

Disclosure of Potential Conflicts of Interest

H-G. Rammensee: ownership interest, BAMOMAB. A. Steinle: ownership interest, BAMOMAB.

Acknowledgments

Received 12/20/2007; revised 4/25/2008; accepted 5/29/2008.

Grant support: Wilhelm-Sander Foundation grant 2004.018.2 and Deutsche Krebshilfe grants 106768 and 107719 (A. Steinle), IZKF Biomat and Deutsche Forschungsgemeinschaft grant Lu869/4-1 (A. Ludwig), and Deutsche Forschungsgemeinschaft grant SFB 685 (S. Stevanovic and H-G. Rammensee).

The costs of publication of this article were defrayed in part by the payment of page charges. This article must therefore be hereby marked *advertisement* in accordance with 18 U.S.C. Section 1734 solely to indicate this fact.

We thank Beate Pömmerl for technical assistance, Jörg Wischhusen for pSuper-puro plasmid, and Kevin Dennehy for critical reading of the manuscript.

References

1. Dunn GP, Old LJ, Schreiber RD. The three Es of cancer immunoediting. Annu Rev Immunol 2004;22:329–60.
2. Smyth MJ, Dunn GP, Schreiber RD. Cancer immunosurveillance and immunoediting: the roles of immunity in suppressing tumor development and shaping tumor immunogenicity. Adv Immunol 2006;90:1–50.
3. Gasser S, Raulet DH. The DNA damage response arouses the immune system. Cancer Res 2006;66:3959–62.
4. Lanier LL. A renaissance for the tumor immunosurveillance hypothesis. Nat Med 2001;7:1178–80.
5. Bauer S, Groh V, Wu J, et al. Activation of NK cells and T cells by NKG2D, a receptor for stress-inducible MICA. Science 1999;285:727–9.
6. Wu J, Song Y, Bakker AB, et al. An activating immunoreceptor complex formed by NKG2D and DAP10. Science 1999;285:730–2.
7. Raulet DH. Roles of the NKG2D immunoreceptor and its ligands. Nat Rev Immunol 2003;3:781–90.
8. Bahram S, Inoko H, Shiina T, Radosavljevic M. MIC and other NKG2D ligands: from none to too many. Curr Opin Immunol 2005;17:505–9.
9. Groh V, Steinle A, Bauer S, Spies T. Recognition of stress-induced MHC molecules by intestinal epithelial γδ T cells. Science 1998;279:1737–40.
10. Welte SA, Sinzger C, Lutz SZ, et al. Selective intracellular retention of virally induced NKG2D ligands by the human cytomegalovirus UL16 glycoprotein. Eur J Immunol 2003;33:194–203.
11. Eagle RA, Trowsdale J. Promiscuity and the single receptor: NKG2D. Nat Rev Immunol 2007;7:737–44.
12. Groh V, Rhinehart R, Secrist H, Bauer S, Grabstein KH, Spies T. Broad tumor-associated expression and recognition by tumor-derived γδ T cells of MICA and MICB. Proc Natl Acad Sci U S A 1999;96:6879–84.
13. Salih HR, Antropius H, Gieseke F, et al. Functional expression and release of ligands for the activating immunoreceptor NKG2D in leukemia. Blood 2003;102:1389–96.
14. Wu JD, Higgins LM, Steinle A, Cosman D, Haugk K, Plymate SR. Prevalent expression of the immunostimulatory MHC class I chain-related molecule is counteracted by shedding in prostate cancer. J Clin Invest 2004;114:560–8.
15. Cerwenka A, Baron JL, Lanier LL. Ectopic expression of retinoic acid early inducible-1 gene (RAE-1) permits natural killer cell-mediated rejection of a MHC class I-bearing tumor *in vivo*. Proc Natl Acad Sci U S A 2001;98:11521–6.
16. Diefenbach A, Jensen ER, Jamieson AM, Raulet DH. Rae1 and H60 ligands of the NKG2D receptor stimulate tumour immunity. Nature 2001;413:165–71.
17. Wiemann K, Mittrucker HW, Feger U, et al. Systemic NKG2D down-regulation impairs NK and CD8 T cell responses *in vivo*. J Immunol 2005;175:720–9.
18. Guerra N, Tan YX, Joncker NT, et al. NKG2D-deficient mice are defective in tumor surveillance in models of spontaneous malignancy. Immunity 2008;28:571–80.
19. Oppenheim DE, Roberts SJ, Clarke SL, et al. Sustained localized expression of ligand for the activating NKG2D receptor impairs natural cytotoxicity *in vivo* and reduces tumor immunosurveillance. Nat Immunol 2005;6:928–37.
20. Smyth MJ, Swann J, Cretney E, Zerafa N, Yokoyama WM, Hayakawa Y. NKG2D function protects the host from tumor initiation. J Exp Med 2005;202:583–8.
21. Doubrovina ES, Doubrovin MM, Vider E, et al. Evasion from NK cell immunity by MHC class I chain-related molecules expressing colon adenocarcinoma. J Immunol 2003;171:6891–9.
22. Groh V, Wu J, Yee C, Spies T. Tumour-derived soluble MIC ligands impair expression of NKG2D and T-cell activation. Nature 2002;419:734–8.
23. Groh V, Smythe K, Dai Z, Spies T. Fas-ligand-mediated paracrine T cell regulation by the receptor NKG2D in tumor immunity. Nat Immunol 2006;7:755–62.
24. Salih HR, Rammensee HG, Steinle A. Cutting edge: down-regulation of MICA on human tumors by proteolytic shedding. J Immunol 2002;169:4098–102.
25. Holdenrieder S, Stieber P, Peterfi A, Nagel D, Steinle A, Salih HR. Soluble MICA in malignant diseases. Int J Cancer 2006;118:684–7.
26. Kaiser BK, Yim D, Chow IT, et al. Disulphide-isomerase-enabled shedding of tumour-associated NKG2D ligands. Nature 2007;447:482–6.
27. Salih HR, Goehlsdorf D, Steinle A. Release of MICB molecules by tumor cells: mechanism and soluble MICB in sera of cancer patients. Hum Immunol 2006;67:188–95.
28. Waldhauer I, Steinle A. Proteolytic release of soluble UL16-binding protein 2 from tumor cells. Cancer Res 2006;66:2520–6.
29. Blobel CP. ADAMs: key components in EGFR signalling and development. Nat Rev Mol Cell Biol 2005;6:32–43.
30. Reiss K, Ludwig A, Saftig P. Breaking up the tie: disintegrin-like metalloproteinases as regulators of cell migration in inflammation and invasion. Pharmacol Ther 2006;111:985–1006.
31. White JM. ADAMs: modulators of cell-cell and cell-matrix interactions. Curr Opin Cell Biol 2003;15:598–606.
32. Maskos K, Fernandez-Catalan C, Huber R, et al. Crystal structure of the catalytic domain of human tumor necrosis factor-α-converting enzyme. Proc Natl Acad Sci U S A 1998;95:3408–12.
33. Mochizuki S, Okada Y. ADAMs in cancer cell proliferation and progression. Cancer Sci 2007;98:621–8.
34. Ludwig A, Hundhausen C, Lambert MH, et al. Metalloproteinase inhibitors for the disintegrin-like metalloproteinases ADAM10 and ADAM17 that differentially block constitutive and phorbol ester-inducible shedding of cell surface molecules. Comb Chem High Throughput Screen 2005;8:161–71.
35. Friese MA, Wischhusen J, Wick W, et al. RNA interference targeting transforming growth factor-β enhances NKG2D-mediated antiglioma immune response, inhibits glioma cell migration and invasiveness, and abrogates tumorigenicity *in vivo*. Cancer Res 2004;64:7596–603.
36. Amour A, Knight CG, English WR, et al. The enzymatic activity of ADAM8 and ADAM9 is not regulated by TIMPs. FEBS Lett 2002;524:154–8.
37. Horiuchi K, Le Gall S, Schulte M, et al. Substrate selectivity of epidermal growth factor-receptor ligand sheddases and their regulation by phorbol esters and calcium influx. Mol Biol Cell 2007;18:176–88.
38. Seals DF, Courtneidge SA. The ADAMs family of metalloproteases: multidomain proteins with multiple functions. Genes Dev 2003;17:7–30.
39. Hundhausen C, Misztela D, Berkhout TA, et al. The disintegrin-like metalloproteinase ADAM10 is involved in constitutive cleavage of CX3CL1 (fractalkine) and regulates CX3CL1-mediated cell-cell adhesion. Blood 2003;102:1186–95.

40. Stoeck A, Keller S, Riedle S, et al. A role for exosomes in the constitutive and stimulus-induced ectodomain cleavage of L1 and CD44. Biochem J 2006;393:609–18.
41. Kenny PA, Bissell MJ. Targeting TACE-dependent EGFR ligand shedding in breast cancer. J Clin Invest 2007;117:337–45.
42. Moss ML, Bartsch JW. Therapeutic benefits from targeting of ADAM family members. Biochemistry 2004; 43:7227–35.
43. van Kempen LC, de Visser KE, Coussens LM. Inflammation, proteases and cancer. Eur J Cancer 2006;42:728–34.
44. Sternlicht MD, Werb Z. How matrix metalloproteinases regulate cell behavior. Annu Rev Cell Dev Biol 2001;17:463–516.
45. Bian J, Wang Y, Smith MR, et al. Suppression of *in vivo* tumor growth and induction of suspension cell death by tissue inhibitor of metalloproteinases (TIMP)-3. Carcinogenesis 1996;17:1805–11.
46. Dulaimi E, Ibanez de Caceres I, Uzzo RG, et al. Promoter hypermethylation profile of kidney cancer. Clin Cancer Res 2004;10:3972–9.
47. Barlaam B, Bird TG, Lambert-Van Der Brempt C, Campbell D, Foster SJ, Maciewicz R. New α-substituted succinate-based hydroxamic acids as TNFα convertase inhibitors. J Med Chem 1999;42:4890–908.
48. Hidalgo M, Eckhardt SG. Development of matrix metalloproteinase inhibitors in cancer therapy. J Natl Cancer Inst 2001;93:178–93.
49. Coussens LM, Fingleton B, Matrisian LM. Matrix metalloproteinase inhibitors and cancer: trials and tribulations. Science 2002;295:2387–92.
50. Fridman JS, Caulder E, Hansbury M, et al. Selective inhibition of ADAM metalloproteases as a novel approach for modulating ErbB pathways in cancer. Clin Cancer Res 2007;13:1892–902.